

NEUTRINO PHYSICS WITH KARMEN*

WOLFGANG KRETSCHMER

for the KARMEN Collaboration[†]

Universität Erlangen–Nürnberg, 91058 Erlangen, Germany

(Received March 7, 2002)

The KARMEN experiment at the pulsed neutron facility ISIS is investigating neutrino–nucleus reactions and neutrino oscillations. In this paper we present cross sections for neutrino induced charged and neutral current reactions on ^{12}C . These results allow a precision test of the standard model of weak interaction by imposing new limits on the neutral current isovector axial vector coupling strength β_A , the strength parameter ρ measuring the universality of W^\pm and Z^0 coupling in the low energy regime and by investigating the Lorentz structure of muon decay. Neutrino oscillations $\bar{\nu}_\mu \rightarrow \bar{\nu}_e$ are investigated in the appearance mode by looking for $p(\bar{\nu}_e, e^+)n$ reactions. An analysis of 3 years running time with the KARMEN2 setup reveals no indication of an oscillation signal excluding most parts of the LSND oscillation evidence.

PACS numbers: 12.15.Mm, 13.15.+g, 14.60.Pq

1. Introduction

The study of neutrino induced processes is interesting from many points of view. Since neutrinos interact via weak interaction only, the investigation of neutrino reactions is best suited for a test of the Standard Model (SM) of electroweak interaction. Many experiments, mostly at high energy, have supported the SM assumptions of lepton number conservation, V–A interaction, flavor universality and the universality of coupling to neutral

* Presented at the TAPS Workshop VI, Krzyże, Poland, September 9–13, 2001.

[†] KARMEN Collaboration: G. Drexlin, K. Eitel, T. Jannakos, M. Kleifges, J. Kleinfeller, C. Oehler, P. Plischke, J. Reichenbacher, M. Steidl, J. Wolf, B. Zeitnitz: Forschungszentrum und Universität Karlsruhe. B.A. Bodmann, E. Finckh, J. Hößl, P. Jünger, W. Kretschmer: Universität Erlangen–Nürnberg. C. Eichner, R. Maschuw, C. Ruf: Universität Bonn. I.M. Blair, J.A. Edgington: Queen Mary and Westfield College, London. N.E. Booth: University of Oxford.

(NC: via Z^0) or charged (CC: via W^\pm) currents. The KARMEN experiment with neutrino energies of up to 52 MeV addresses most of these topics by the investigation of neutrino induced reactions on ^{12}C . Since the energies of the ISIS neutrinos are very similar to those originating from a supernova, the cross sections obtained in the KARMEN experiment are important both for the understanding of neutrino induced element synthesis and for detector design for the measurement of supernova neutrinos. The second topic of KARMEN is the investigation of neutrino oscillations, which violate the lepton number conservation and which would be an evidence for a neutrino mass. In 1996 the LSND collaboration reported a positive neutrino oscillation result [1] which prompted our collaboration to modify the detector by adding another layer of active anti-counter. In this way the sensitivity of KARMEN to oscillations is enhanced considerably, the results will be presented in Section 4.

2. The KARMEN experiment

The KARMEN experiment is performed at the neutron spallation facility ISIS of the Rutherford Appleton Laboratory. From a 50 Hz Rapid Cycling Synchrotron an 800 MeV, 200 μA pulsed proton beam hits a Ta/D₂O spallation target. Apart from neutrons used for condensed matter research, also a large number of pions are produced in the spallation process. The π^- are absorbed by the target nuclei whereas the π^+ Decay At Rest (DAR). Muon neutrinos ν_μ emerge from the decay $\pi^+ \rightarrow \mu^+ + \nu_\mu$. The low energy μ^+ are also stopped within the massive target and decay via $\mu^+ \rightarrow e^+ + \nu_e + \bar{\nu}_\mu$. Due to this $\pi^+ - \mu^+$ decay chain at rest ISIS represents a neutrino source with identical intensities for ν_μ , ν_e and $\bar{\nu}_\mu$ emitted isotropically with a flux of 6.37×10^{13} ν/s per flavor for a proton beam current of 200 μA . There is only a very small intrinsic contamination of $\bar{\nu}_e/\nu_e \leq 6.2 \times 10^{-4}$ [2] from π^- decay in flight followed by μ^- DAR which is further reduced by evaluation cuts but has to be taken into account as a background to the oscillation channel under consideration.

The energy spectra of the neutrinos are well defined due to DAR of both the π^+ and μ^+ (Fig. 1(a)). The ν_μ are monoenergetic with an energy of 29.8 MeV, the continuous energy distributions of ν_e and $\bar{\nu}_\mu$ up to 52.8 MeV can be calculated using V-A theory. A unique feature of the ISIS neutrino source is the time structure of the neutrinos which is closely related to that of the proton beam showing two pulses of 100 ns base width 225 ns apart with a repetition frequency of 50 Hz. Due to the short life time of π^+ , $\tau = 26$ ns, there are two prompt bursts of monoenergetic ν_μ within the first 500 ns (Fig. 1(b)). In a time window from 0.5 μs to 10 μs , when all ν_μ have vanished already, one is left with ν_e and $\bar{\nu}_\mu$ showing the characteristic

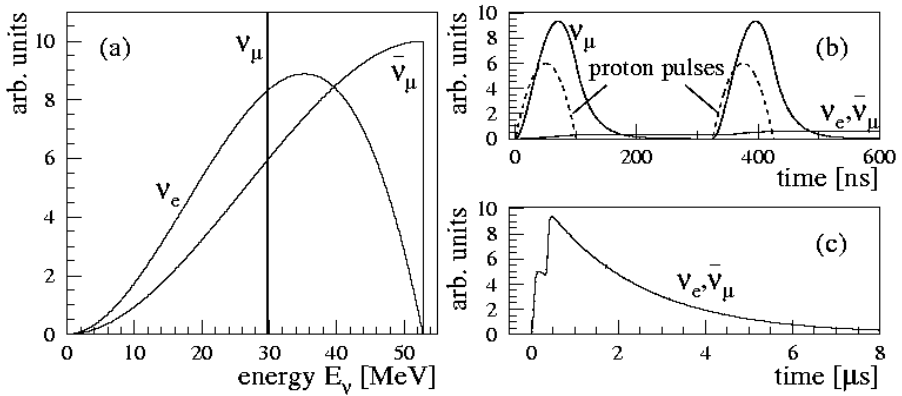


Fig. 1. Neutrino energy spectra (a) and time distribution of ν_μ (b) and $\nu_e, \bar{\nu}_\mu$ (c) at ISIS.

exponential time slope of 2.2 μ s from its producing μ^+ decay (Fig. 1(c)). This different time structure allows a clear separation of the ν_μ burst from the following ν_e and $\bar{\nu}_\mu$ by applying appropriate time cuts, the duty cycle of 10^{-4} enables an effective suppression of cosmic background. The neutrinos are detected in a rectangular tank filled with 56 tons of liquid scintillator [3] which consists entirely of hydrocarbons and thus serves as a massive life target for the investigation of neutrino interactions with ^{12}C . The scintillation calorimeter is segmented by totally reflecting double lucite sheets into 512 independent modules, where the scintillation light is transported to both ends of the module and registered by two Photo Multipliers (PM). The event position is determined by the hit module and the time difference of the PM signals, the time resolution is 1 ns and the energy resolution is $\Delta E/E = 12\%/\sqrt{E(\text{MeV})}$. A Gd_2O_3 coated paper within the module sheets provides efficient detection of thermal neutrons due to the very high capture cross section of the $\text{Gd}(n, \gamma)$ reaction ($\sigma \approx 49000$ barn) in addition to the $p(n, \gamma)d$ capture. The KARMEN electronics is synchronized to the ISIS proton pulses to an accuracy of better than ± 2 ns, so that the time structure of the neutrino induced events can be exploited in full detail.

A massive blockhouse of 7000 t of steel in combination with a system of two layers of active veto counters provide shielding against beam correlated spallation neutron background, suppression of the hadronic component of cosmic radiation as well as reduction of the cosmic muon flux. In 1996 an additional third veto counter system with a total area of 300 m^2 was installed within the 3 m thick roof and the 2–3 m thick walls of iron shielding [4] (KARMEN2 experimental configuration). By detecting muons which pass through the steel at a distance of less than one meter from the de-

tector and, therefore, vetoing the successive energetic neutrons from deep inelastic scattering and μ^- capture in iron, the main background for the $\bar{\nu}_\mu \rightarrow \bar{\nu}_e$ oscillation search could be reduced by a factor of 40 compared to the KARMEN1 setup.

3. Neutrino–nucleus reactions

3.1. Electroweak transitions in the mass 12 system

The physics potential of KARMEN for the investigation of neutrino–nucleus interaction can best be demonstrated referring to Fig. 2. It shows the CC and NC electroweak transitions between the ground state of ^{12}C and the isobaric analogue triplet states of the $A = 12$ system *i.e.* ^{12}B , $^{12}\text{C}^*$, and ^{12}N . These transitions between nuclear states serve as a spin–isospin filter for the investigation of specific components of the weak hadronic current. In this particular case, with simultaneous spin- and isospin-flip, $\Delta T = \Delta S = 1$, the isovector–axialvector coupling dominates both, the CC and NC reactions.

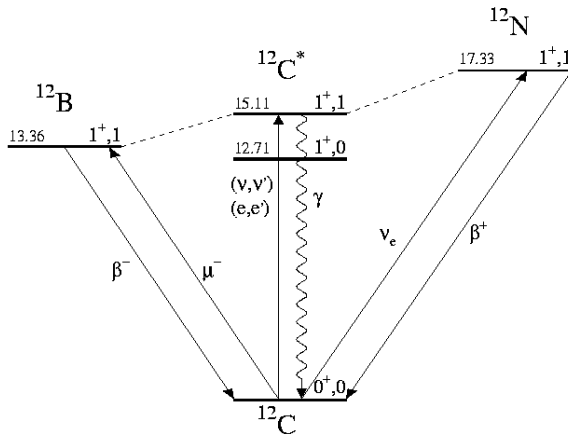


Fig. 2. The $A = 12$ isobaric analogue triplet.

In the KARMEN experiment cross sections for charged current reaction $^{12}\text{C}(\nu_e, e^-)^{12}\text{N}_{\text{g.s.}}$ and, for the first time, for the neutral current nuclear excitation $^{12}\text{C}(\nu, \nu')^{12}\text{C}^*(1^+ 1; 15.1 \text{ MeV})$ initiated by ν_μ and ν_e , $\bar{\nu}_\mu$, respectively, have been measured with spectroscopic quality. The investigation of these reactions is ideally suited for a study of specific parts of the weak hadronic current and thus for a determination of special coupling constants. These involve the isovector–axialvector coupling constant β_A representing the strength of the amplitude $[\bar{u}\gamma_\lambda\gamma^5 u - \bar{d}\gamma_\lambda\gamma^5 d]$ and the overall strength

parameter ρ [5] of neutral current interaction which are both predicted to be one in the standard model. Another test of the standard model can be performed by investigating the energy spectrum of the ν_e emitted in the decay $\mu^+ \rightarrow e^+ + \nu_e + \bar{\nu}_\mu$ of muons produced in the beam stop of the ISIS source. In this way the shape parameter ω_L of the ν_e spectrum, which depends on vector, scalar and tensor components of the weak interaction, can be deduced. In the SM all non V–A components vanish and ω_L is predicted to be 0.

On the other hand the exact knowledge of neutrino–nucleus cross sections and their reliable theoretical description is essential for the investigation of neutrino induced nucleosynthesis in supernova explosions where the energy spectra of neutrinos with temperatures of about 5 MeV for ν_e and about 10 MeV for ν_μ , respectively, cover the same range as the ISIS neutrino source.

3.2. Exclusive CC reaction $^{12}\text{C}(\nu_e, e^-)^{12}\text{N}_{g.s.}$

The most stringent signature for a neutrino induced reaction at KARMEN is provided by the CC inverse β decay reaction $^{12}\text{C}(\nu_e, e^-)^{12}\text{N}_{g.s.}$ with a Q value of 17.3 MeV. The signature of this reaction is a spatially correlated delayed coincidence of a prompt electron with kinetic energies $E_{e^-} \leq 35.5$ MeV within 0.5 to 10 μs after beam on target and a positron with $E_{e^+} \leq 16.3$ MeV from the subsequent β^+ decay of $^{12}\text{N}_{g.s.}$ from 0.5 to 36 ms. The positron from the ^{12}N decay uniquely identifies ν induced transitions to the ground state since excited states are particle unstable and will not be seen in the scintillation detector due to much lower light output of hadronic energy loss. After appropriate software cuts on time, energy and position correlation and a pre-trigger veto to the sequence in case of any cosmic ray activity in a 20 μs interval preceding the prompt or delayed event a total of 870 correlated events with complete signature remain. The corresponding background measured in the beam pause was only 17.5 events which gives a signal to background ratio of 50 to 1. The quality of the data is reflected in Fig. 3. The time distribution of the prompt signal (Fig. 3(c)) which is well described by a decay constant of 2.2 μs , clearly demonstrates that these events are induced by ν_e originating from μ^+ decay. The measured energy spectrum (Fig. 3(a)) also agrees with the expected electron energy distribution from the $^{12}\text{C}(\nu_e, e^-)^{12}\text{N}_{g.s.}$ reaction. The same agreement for the time and energy spectra of the delayed signal is found with those expected from the ^{12}N decay (Fig. 3(b), 3(d)). From these almost background free data a cross section averaged over the energy distribution of the DAR ν_e spectrum was deduced to be

$$\langle \sigma(^{12}\text{C}(\nu_e, e^-)^{12}\text{N}_{g.s.}) \rangle = [9.5 \pm 0.3(\text{stat.}) \pm 0.8(\text{syst.})] \times 10^{-42} \text{cm}^2.$$

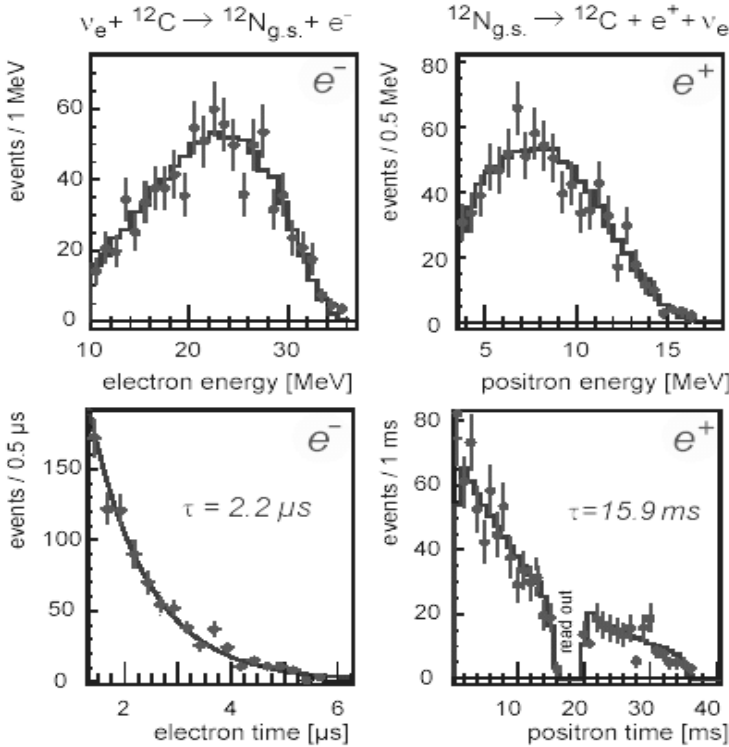


Fig. 3. Energy and time spectra of the prompt and delayed signal from the reaction $^{12}\text{C}(\nu_e, e^-)^{12}\text{N}_{\text{g.s.}}$ and the subsequent β^+ decay of $^{12}\text{N}_{\text{g.s.}}$.

This value is in excellent agreement with theoretical approaches using either one body density shell model approach (OBD) [6, 7], Continuum Random Phase Approximation (CRPA) [8] or the Elementary Particle Treatment (EPT) [9, 10], all ranging from $(8.9\text{--}9.4)\times 10^{-42}\text{cm}^2$ and with the recent LSND experiment [11].

3.3. The neutral current reactions $^{12}\text{C}(\nu, \nu')^{12}\text{C}^*(1^+ 1; 15.1\text{MeV})$

The neutrino induced NC excitation of nuclei has been observed for the first time by KARMEN in the reaction $^{12}\text{C}(\nu, \nu')^{12}\text{C}^*(1^+ 1; 15.1\text{MeV})$ [12, 13], induced by ν_e and $\bar{\nu}_\mu$. The signature of this reaction is a localized scintillation event of 15.1 MeV from the γ -ray de-excitation of the excited $^{12}\text{C}^*$ level to the ground state with a branching ratio of $(92 \pm 2)\%$. With the time slot of the ν_e and $\bar{\nu}_\mu$, *i.e.* $0.5\mu\text{s} \leq t \leq 10\mu\text{s}$ the energy spectrum of single prong events in the central detector as shown in Fig. 4 is obtained. This spectrum shows a prominent peak between 11 and 16 MeV, attributed to the inelastic

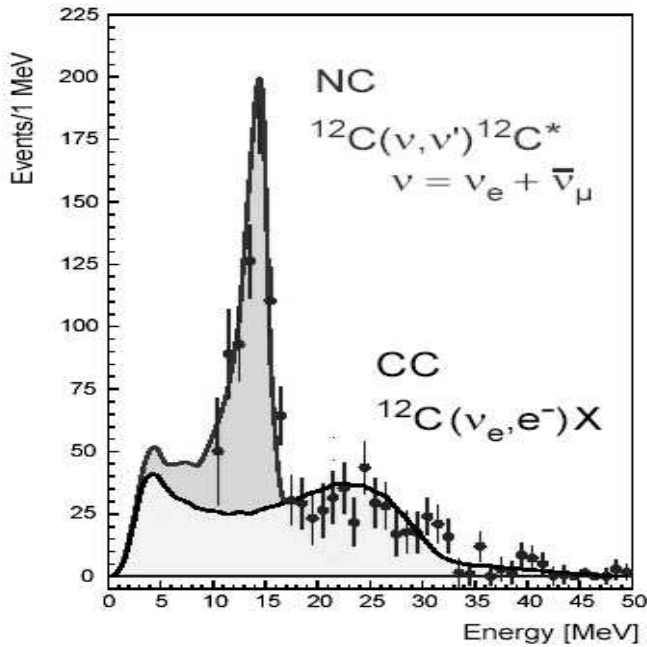


Fig. 4. Energy spectrum in the ν_e , $\bar{\nu}_\mu$ -time window, the peak around 15 MeV corresponds to the reaction $^{12}\text{C}(\nu, \nu')^{12}\text{C}^*$.

NC scattering process $^{12}\text{C}(\nu, \nu')^{12}\text{C}^*(1^+ 1; 15.1 \text{ MeV})$ induced by both, ν_e and $\bar{\nu}_\mu$. The time distribution of single prong events with energies above 10 MeV is consistent with a $2.2 \mu\text{s}$ decay time, which clearly demonstrates the neutrino induced nature of the observed signals. The broad distribution of events with energies above 17 MeV, which have the same time dependence, consists of contributions from four reactions: neutrino–electron scattering, and the CC reactions $^{13}\text{C}(\nu_e, e^-)^{13}\text{N}$, $^{12}\text{C}(\nu_e, e^-)^{12}\text{N}^*$ and $^{12}\text{C}(\nu_e, e^-)^{12}\text{N}_{\text{g.s.}}$ (where the subsequent β^+ decay is not observed). For a Maximum Likelihood (ML) analysis of the whole spectrum the small contribution from $\nu - e$ scattering was taken from literature and the events due to $^{12}\text{C}(\nu_e, e^-)^{12}\text{N}_{\text{g.s.}}$ were taken from the exclusive measurement described before (in Fig. 4 these events are already subtracted). The remaining CC reactions together with the NC excitation on ^{12}C were analyzed with the ML method resulting in 533 ± 34 NC events from which the NC cross section averaged over the energy spectra of ν_e and $\bar{\nu}_\mu$ was obtained

$$\langle \sigma(^{12}\text{C}(\nu, \nu')^{12}\text{C}^*) \rangle = [10.9 \pm 0.7(\text{stat.}) \pm 0.8(\text{sys.})] \times 10^{-42} \text{ cm}^2.$$

As for the exclusive CC reaction discussed before, there is excellent agreement with corresponding theoretical calculations [6–10] ranging from $(9.8\text{--}11.9)\times 10^{-42}\text{ cm}^2$.

For the investigation of the ν_μ induced NC excitation the time window 0–600 ns after beam on target has to be used. The ν_μ -induced reactions have to be disentangled from background events originating from cosmic muons and from beam correlated neutrons. In addition there are some events due to $(\nu_e + \bar{\nu}_\mu)$ reactions from μ^+ decay and some due to ν_μ -e scattering. Fig. 5 shows both time and energy distribution of measured events compared to

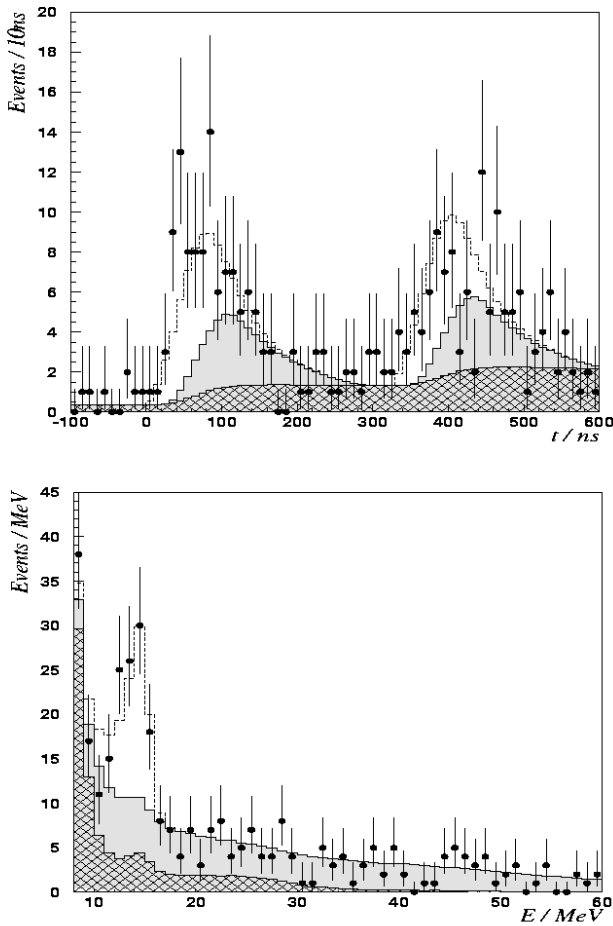


Fig. 5. Time (top) and energy (bottom) distribution of measured events compared to ML fit (dashed line). Hatched area: cosmic background and contributions of $(\nu_e + \bar{\nu}_\mu)$ induced reactions, shaded area: fast neutron background, white area: muon neutrino events.

a maximum likelihood fit. As can be seen in the upper part of Fig. 5, the earlier parts of the double bunches are dominated by neutrino events whereas the later parts (shaded area) are dominated by fast neutron events. In a maximum likelihood analysis the ν_μ induced events are separated from these neutron events and from the contribution due to $(\nu_e + \bar{\nu}_\mu)$ reactions. After subtracting calculated 3 events due to ν_μ - e scattering 86 ± 15 NC events remain, corresponding to a cross section at a ν_μ energy of 29.8 MeV of [14]

$$\sigma(^{12}\text{C}(\nu_\mu, \nu_\mu')^{12}\text{C}^*) = [3.2 \pm 0.5(\text{stat.}) \pm 0.4(\text{syst.})] \times 10^{-42} \text{cm}^2.$$

Again there is good agreement with theoretical calculations [6–10] ranging from $(2.64\text{--}2.80) \times 10^{-42} \text{cm}^2$. This overall good agreement of the both NC reactions with theory clearly demonstrates that the NC excitation on ^{12}C may be appropriate for the development of future detectors for the bolometric measurement of supernova neutrinos, since it is sensitive to all neutrino species. The implications of these CC and NC neutrino cross sections on the coupling constants β_A and ρ will be discussed in the following section.

3.4. Test of standard model predictions

As mentioned before in Section 3.1 the neutrino reactions within the $A = 12$ system can be used to determine β_A and ρ which are both predicted to be 1 in the standard model. The cross sections for the investigated spin- and isospin-changing NC and CC reactions can be written according to Ref. [6] as a sum of doubly reduced matrix elements taking into account proper spin- and isospin-coupling and including the coupling strength parameters explicitly. The reaction is mediated by four different one-body operators representing multiple projections of the charge, longitudinal and two transverse parts of the four-current (vector and axial-vector parts). The doubly-reduced matrix elements of any one-body operator, $\hat{T}_{J,T}(\mathbf{q}^2)$, such as the multiple operators involved in semi-leptonic weak and electromagnetic interactions, can be written as

$$\langle J_f, T_f || \hat{T}_{J,T}(\mathbf{q}^2) || J_i, T_i \rangle = \sum_{a \geq b} \chi_{J,T}^{(\text{fi})}(a, b) \langle a || T_{J,T}(\mathbf{q}^2) || b \rangle,$$

where a, b are single particle quantum numbers $\{n, l, j\}$ and $\chi_{J,T}^{(\text{fi})}(a, b)$ are real coefficients labeled by the rank J, T of the tensor, by the single particle quantum numbers a, b and by (fi) which signifies the involved final and initial states. Due to the truncated single particle space the number of coefficients $\chi_{J,T}^{(\text{fi})}(a, b)$ is small enough to be determined from experimental results from ^{12}N and ^{12}B β decay, μ -capture on ^{12}C , and inelastic electron

scattering on ^{12}C . For the calculation of the single particle matrix elements harmonic oscillator wave functions have been used. Using these coefficients the integrated neutrino cross sections for the CC and NC reactions on ^{12}C can be deduced

$$\sigma_{\text{NC}} = \rho^2(c_2\beta_A^2 + c_1\beta_A + c_0), \quad \sigma_{\text{CC}} = d_2\beta_A^2 + d_1\beta_A + d_0,$$

where the parameters c_i and d_i are calculated in the model mentioned above. Before comparing it to the integrated cross sections the continuous energy distributions of ν_e and $\bar{\nu}_\mu$ originating from muon decay and the experimental energy resolution have to be taken into account. The isovector–axialvector coupling constant was deduced from the exclusive CC neutrino cross section (Section 3.2) to be $\beta_A = 0.99 \pm 0.06$.

TABLE I

Isvector–axialvector coupling constant obtained from high energy experiments in comparison with the derived value from KARMEN.

Experiment	$ \beta $	Reference
Aachen–Padova	0.93 ± 0.12	[16]
CHARM	1.10 ± 0.23	[17]
SKAT	0.99 ± 0.20	[18]
FNAL-15	0.98 ± 0.24	[19]
KARMEN	0.99 ± 0.06	[15]

The quoted error was obtained from the experimental uncertainty of the neutrino cross section and from a Monte Carlo variation of the coefficients $\chi_{J,T}^{(\hat{n})}(a, b)$ to reproduce the β^\pm decay within the $A = 12$ multiplet and the μ capture on ^{12}C within their errors, more details can be found in the thesis of Bodmann [15]. This result is in complete agreement with high energy experiments in the GeV range, where $|\beta|$ was deduced from coherent π^0 production in neutrino reactions on nuclei, and thus provides a further confirmation of the standard model even at very low energies.

The strength parameter ρ of the neutral current interaction was deduced from the ratio of NC to CC cross section using both neutral current cross sections (ν_μ and ν_e , $\bar{\nu}_\mu$ induced): $\rho = 1.02 \pm 0.04$ [15]. As in the case of β_A the quoted error takes into account the experimental uncertainties of both, the KARMEN neutrino cross sections and the β^\pm decay and μ -capture,

respectively. This result is another confirmation of the standard model at low energies and it is in agreement with the world average of $\rho = 0.9998 \pm 0.0011$ [20], obtained from multi-GeV experiments only.

The shape parameter ω_L of the ν_e spectrum from μ^+ decay was determined by analyzing the energy distribution of electrons produced in the reaction $^{12}\text{C}(\nu_e, e^-)^{12}\text{N}_{\text{g.s.}}$. As the recoil energy of the ^{12}N nucleus is negligible, the ν_e energy E_ν is deduced from the measurement of the electron energy E_e via the kinematic relation $E_\nu = E_e + Q$, where $Q = 17.3$ MeV is the Q value of the detection reaction. The energy dependence of the cross section is dominated by the space phase factor $(E_\nu - Q)^2$. Therefore, a low rate of additional ν_e near the kinematic end point $E_{\text{max}} = 52.8$ MeV (and less ν_e for $E < 40$ MeV) due to non-standard couplings is translated to the observation of a higher rate of electrons for $E_e > 20$ MeV and thus to a distortion of the visible energy spectrum. A maximum likelihood analysis was carried out on an event-by-event basis for several fit intervals with a result of $\omega_L = 0.027 \pm 0.038(\text{stat.}) \pm 0.031(\text{syst.})$ corresponding to an upper limit $\omega < 0.113$ at 90% confidence limit, indicating no evidence for non V-A components in muon decay. More details of the analysis and the consequences for scalar and tensor amplitudes in μ decay are described in detail in Ref. [21].

4. Neutrino oscillations

Other non-standard model processes are neutrino oscillations among neutrinos of different flavors with $\Delta L = 0$, but violating family lepton numbers L_e and L_μ . Such oscillations imply massive neutrinos with non-degenerate masses, the relevant parameters for the oscillation probability in a 2 flavor scheme are the mixing angle Θ and the difference Δm^2 of the masses squared. In this contribution we only discuss the $\bar{\nu}_\mu \rightarrow \bar{\nu}_e$ oscillation search in the appearance mode, since KARMEN is most sensitive to this oscillation channel. The signature for the detection of $\bar{\nu}_e$ is a spatially correlated delayed coincidence of positrons from $p(\bar{\nu}_e, e^+)n$ with energies up to $E_{e^+} = E_{\bar{\nu}_e} - Q = 52.8 - 1.8 = 51.0$ MeV and γ -emission of either of the two capture processes $p(n, \gamma)d$ with one γ of 2.2 MeV or $\text{Gd}(n, \gamma)$ with 3 γ -quanta on average with a sum energy of 8 MeV (Fig. 6). The shape of the expected positron energy spectrum depends on Δm^2 , reflecting the Δm^2 dependence of the oscillation probability. The positrons are expected in a time window of several μs after beam on target with a 2.2 μs exponential decrease due to the μ^+ decay, the time difference between the e^+ and the capture γ is given by the thermalization, diffusion and capture of the neutrons, $\tau_n \approx 110 \mu\text{s}$. The data analyzed in this oscillation search were taken since the commissioning of the new veto in February 1997 until March 2000, in total 7160 C protons-on-target have been accumulated corresponding to

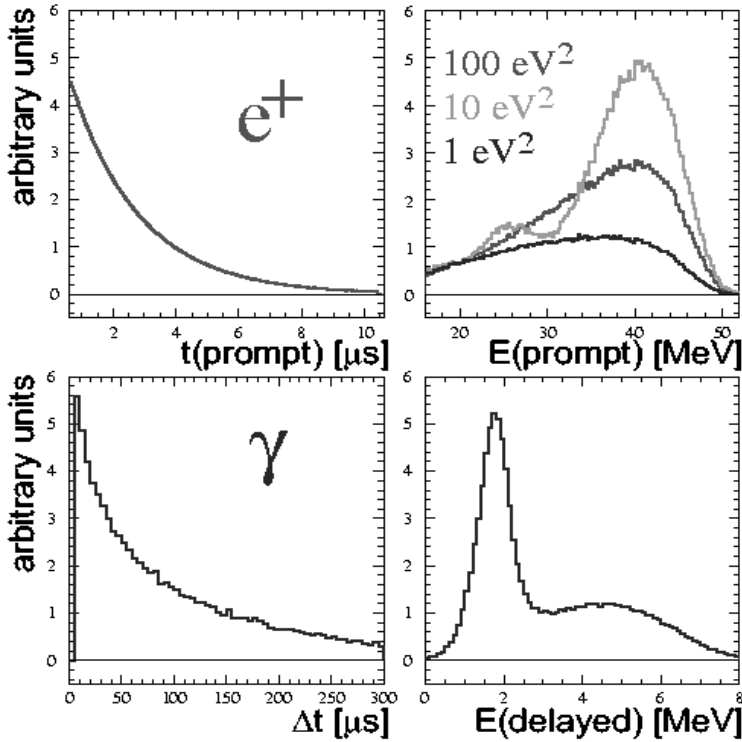


Fig. 6. Expected sequences from an oscillation signal: simulated time and energy spectra of e^+ and correlated γ -events.

$2.1 \times 10^{21} \bar{\nu}_\mu$. A prompt positron event is accepted only if there is neither previous activity in the central detector nor in the two inner veto counters, the required cuts are $0.6\text{--}10.6 \mu\text{s}$ in time and $16\text{--}50 \text{ MeV}$ in energy. The cuts for the delayed expected neutron signal is $5\text{--}300 \mu\text{s}$ for the time difference, $\leq 8 \text{ MeV}$ for the energy and a volume of 1.3 m^3 for the spatial coincidence. These cuts lead to a small sample of 11 sequences, their time and energy distribution are shown in Fig. 7, compared to expected background from different sources. The total background for $\bar{\nu}_e$ search within the evaluation cuts is listed in Table II, the last line shows the expected sequential events for maximal mixing and $\Delta m^2 \geq 100 \text{ (eV}/c^2)^2$. The first three background components are determined precisely during the normal measurements: the cosmic background is measured with high statistics in the long pre-beam window, the ν induced background is measured with KARMEN in different time and energy windows. Only the small intrinsic ISIS $\bar{\nu}_e$ contribution from π^- decaying in flight has to be simulated [2]. It is a remarkable success of the KARMEN upgrading that the cosmic background amounts to about

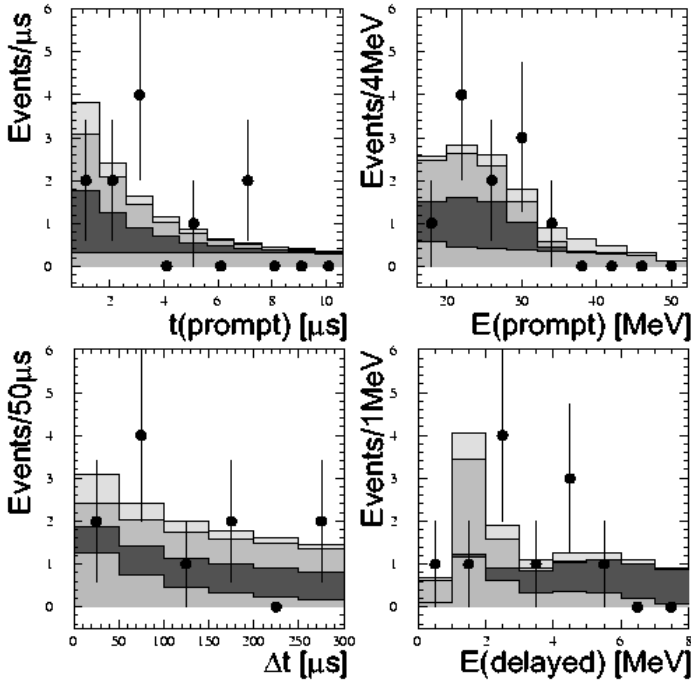


Fig. 7. Spectra of the 11 candidate events after applying all cuts compared to the expected background contributions (from bottom to top): cosmic background, (e^-, e^+) from $^{12}\text{C}(\nu_e, e^-)^{12}\text{N}_{\text{g.s.}}$, ν induced random coincidences and ISIS $\bar{\nu}_e$ contamination.

TABLE II

Total background expectation for $\bar{\nu}_e$ search within the evaluation cuts. Last line: oscillation expectation for maximal mixing.

Background contribution	Events
Cosmic induced sequences	3.2 ± 0.2
(e^-, e^+) from $^{12}\text{C}(\nu_e, e^-)^{12}\text{N}_{\text{g.s.}}$	3.9 ± 0.5
ν induced random coincidences	3.5 ± 0.3
ISIS $\bar{\nu}_e$ contamination	1.7 ± 0.2
Total background	12.3 ± 0.6
$\bar{\nu}_e$ signal for $\sin^2(2\theta) = 1$	2442 ± 269

25% of the total background only. The 11 candidate events are in good agreement with the total background expectation of 12.3 ± 0.6 , from which an upper limit of $N(\text{osc}) \leq 6.3$ at 90% CL can be extracted using a Bayesian approach. Comparison of the measured sequences with the background time and energy spectra (Fig. 7) show no obvious deviations. A more sensitive method to extract a possible $\bar{\nu}_\mu \rightarrow \bar{\nu}_e$ signal or to prove the no-oscillation hypothesis is the maximum likelihood analysis which is possible due to the very good resolution of the KARMEN detector in time, energy and position. The ML analysis takes into account a precise spectral knowledge of all

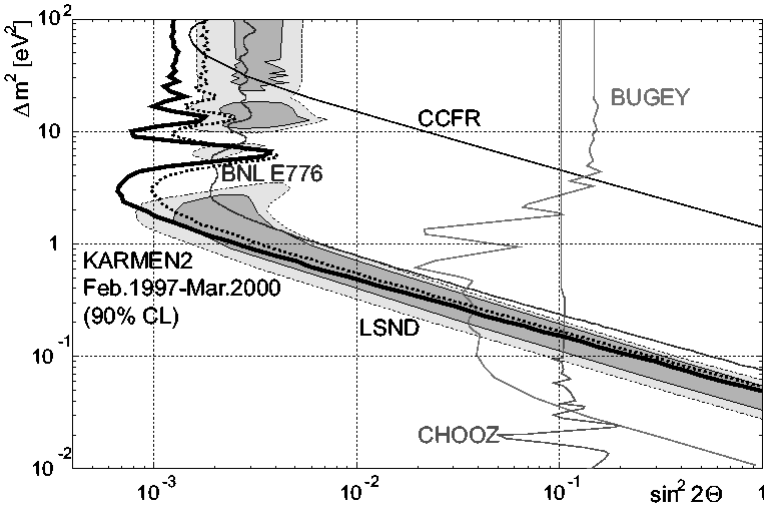


Fig. 8. KARMEN2 exclusion limit and sensitivity (dashed curve) at 90 % CL compared to other experiments: BNL E776 [22], CCFR [23], BUGEY [24], CHOOZ [25] and the evidence for $\bar{\nu}_\mu \rightarrow \bar{\nu}_e$ oscillations reported by LSND [26].

background sources and a detailed Monte Carlo description of the oscillation signature in the detector. The likelihood function is optimized with respect to the unknown parameters Δm^2 and $\sin^2(2\theta)$ using the following signatures: time and energy of prompt and delayed event and spatial correlation between both events. With the current KARMEN2 data there is no hint for an $\bar{\nu}_\mu \rightarrow \bar{\nu}_e$ oscillation signal. To deduce exclusion plots for Δm^2 and $\sin^2(2\theta)$ a unified approach suggested by Feldmann and Cousins [27] has been applied. The KARMEN2 exclusion limit (90 % CL) is shown in Fig. 8 compared to the limits from other experiments, [22, 25], and to the favored regions from LSND based on a complete reanalysis of the entire 1993–1998 data set [26]. The dark (light) shaded area of the latter corresponds to an evidence at 90% (99%) CL. At high Δm^2 , KARMEN completely excludes the

region favored by LSND, below $1(\text{eV}/c^2)^2$ it leaves some statistical space, but the reactor experiments at Bugey and Chooz add stringent limits from the $\bar{\nu}_e$ disappearance search.

As a conclusion, there is not much parameter space left from the LSND evidence, but a common analysis of LSND and the full KARMEN2 data set seems to be necessary to deduce more stringent limits on the allowed parameter region for neutrino oscillations. KARMEN has stopped data taking in April 2001, having seen no hints for neutrino oscillations so far, a further cross-check of the LSND parameter region will be performed by the upcoming BooNE experiment at Fermilab.

We gratefully acknowledge the financial support from the German Bundesministerium für Bildung, Wissenschaft, Forschung und Technologie (BMBF), the Particle Physics and Astronomy Research Council (PPARC), and the Central Laboratory of the Research Council (CLRC).

REFERENCES

- [1] C. Athanassopoulos *et al.*, *Phys. Rev.* **C54**, 2685 (1996).
- [2] R.L. Burman *et al.*, *Nucl. Instrum. Methods Phys. Res.* **A368**, 416 (1996).
- [3] G. Drexlin *et al.*, *Nucl. Instrum. Methods Phys. Res.* **A289**, 490 (1990).
- [4] G. Drexlin *et al.*, *Prog. Part. Nucl. Phys.* **40**, 193 (1998).
- [5] P.Q. Hung, J.J. Sakurai, *Ann. Rev. Nucl. Part. Sci.* **31**, 375 (1981).
- [6] T.W. Donnelly, *Phys. Lett.* **B43**, 93 (1973).
- [7] J. Engel *et al.*, *Phys. Rev.* **C54**, 2740 (1996).
- [8] E. Kolbe *et al.*, *Phys. Rev.* **C49**, 1122 (1994).
- [9] M. Fukugita *et al.*, *Phys. Lett.* **B212**, 139 (1988).
- [10] S.L. Mintz *et al.*, *Phys. Rev.* **C40**, 2458 (1989).
- [11] C. Athanassopoulos *et al.*, *Phys. Rev.* **C55**, 2078 (1997).
- [12] B. Bodmann *et al.*, *Phys. Lett.* **B267**, 321 (1991).
- [13] B.E. Bodmann *et al.*, *Phys. Lett.* **B332**, 251 (1994).
- [14] B. Armbruster *et al.*, *Phys. Lett.* **B423**, 15 (1998).
- [15] B.A. Bodmann, Ph.D. thesis, Erlangen 2002.
- [16] H. Faissner *et al.*, *Phys. Lett.* **B125**, 230 (1983).
- [17] F. Bergsma *et al.*, CHARM Collaboration, *Phys. Lett.* **B157**, 469 (1985).
- [18] H.J. Grabosch *et al.*, SKAT Collaboration, *Z. Phys.* **C31**, 203 (1986).
- [19] C. Baltay *et al.*, *Phys. Rev. Lett.* **57**, 2629 (1986).
- [20] Particle Data Group, *Eur. Phys. J.* **C15**, 103 (2000).
- [21] B. Armbruster *et al.*, *Phys. Rev. Lett.* **81**, 520 (1998).

- [22] L. Borodovsky *et al.*, *Phys. Rev. Lett.* **68**, 274 (1992).
- [23] A. Romosan *et al.*, *Phys. Rev. Lett.* **78**, 2912 (1997).
- [24] B. Achkar *et al.*, *Nucl. Phys.* **B434**, 503 (1995).
- [25] M. Apollonio *et al.*, *Phys. Lett.* **B348**, 19 (1995).
- [26] I. Stancu, Proc. Int. Workshop on Neutrino Telescopes, Ed. M. Baldo Ceolin, Venice 2001; A. Aguilar *et al.*, [hep-ex/0104049](#).
- [27] G. Feldmann, R. Cousins, *Phys. Rev.* **D57**, 3873 (1998).